Investigating the Ageing Effects on Image Sensors Due to Terrestrial Cosmic Radiation

Gayathri G. Nampoothiri [1], Albert J. P. Theuwissen [1, 2]
[1] Delft University of Technology, Mekelweg 4
2628 CD, Delft, the Netherlands
[2]Harvest Imaging, Bree, Belgium
Phone: +31 (0)15 2787534, G.GangadharanNampoothiri@tudelft.nl

INTRODUCTION

Gray hair and balding are considered to be the signs of ageing in humans. Imagers too exhibit a tendency to age which manifests as the generation of hard errors such as increase in hot spots, dark current etc even during on-the-shelf storage. It is hypothesized that the ageing phenomenon is due to the influence of terrestrial cosmic rays [1], which are the result of very high energy particles created in space, which hit the earth's stratosphere to produce secondary particles [2]. To validate this hypothesis and understand the phenomenon better, measurements were carried out on devices stored on-the-shelf, on those carried around the world in airplanes, and also on devices kept running on the camera.

EXPERIMENTAL SETUP AND DEVICE USED

Measurement setup consists of a signal-processing board, a sensor board holding 16 imagers in parallel, an oven, a frame grabber, a laptop and LABView programs capable of measuring 16 CCD's simultaneously. The experimental device used is a frametransfer CCD measured as a full frame with an active area of 8.8 x 6.6 mm^2 and pixel size of $9\mu m \times 22\mu m$ in the image section and $9\mu m \times 18.6\mu m$ in the storage.

EVALUATION METHOD

To expose the sensors to "natural radiation" at high altitudes, they were shipped from Amsterdam to San Francisco back and forth by aircraft for a total flight time of approximately one day. Pre- and post-flight measurements were carried out. Reference sensors kept on the shelf at room temperature (mentioned hereafter as reference sensors) and sensors kept running on the camera (mentioned hereafter as free running sensors) were measured at regular intervals for comparison. All measurements are done at 32 degree Celsius and with an integration time of 3 seconds.

The newly generated hot pixels as well as the increase in the amplitude of the existing leaky pixels post-flight are clearly visible from Fig. 1. The amplitude of the pixel is expressed in digital numbers (DN). Most of the pixels form a nearly Gaussian distribution with a mean value between 100 and 120 DN (Fig. 2). Pixels with values eight times higher than the standard deviation is marked out as a hot pixel and their amplitude is recorded. This experiment is repeated for the test, reference and free running sensors. Fig. 3 shows the result obtained from such a measurement cycle. The number of hot pixels generated is highest in the case of test sensors and there is a slight shift of the curve towards the right indicating an increase in the amplitude of the hot pixels. Transporting sensors by aircraft from Amsterdam to San Francisco brings them to high altitude (33,000 ft). The energy and density of cosmic rays is dependant on altitude, latitude as well as the earth's magnetic field [2]. The probability of developing hot pixels with large amplitudes is relatively higher for the test sensor compared to that of the reference sensor or the free running sensor (Fig. 4). Arrhenius plots (Fig. 5) of the dark current performed on pre-and post-flight

sensors yielded their respective activation energies. Table.1 gives the extracted activation energy in eV. At low temperatures, the energy available to the electrons is too low for them to overcome the band gap directly, and excitation involving impurities is dominant [3]. This results in activation energy of approximately Eg/2. A decrease in average activation energy of about 5% is noted post-flight. A larger decrease in activation energy is observed for individual hot pixels post flight (Fig. 6, Table. 2). This maybe due to the bulk damage caused by the neutrons present in the terrestrial cosmic rays. The energy of terrestrial cosmic ray is high enough to displace silicon atom from its lattice position forming an interstitial and vacancy pair called Frenkel pair [4]. Most pairs recombine and the remaining vacancies migrate to form stable defect [5]. These defects also interact with impurities to form defect-impurity complexes which give rise to states with energy levels in the forbidden band gap [6]. The lowering of the average activation energy of the sensor post-flight is most likely due to the lowering of hot pixel activation energy.

CONCLUSIONS

1. Sensors transported by aircraft showed the maximum increase in the probability to create hot pixels.
2. Hot pixels with large amplitude seem to suffer more from damage due to terrestrial cosmic radiation.
3. Activation energy approximately equal to Eg /2 is obtained. However a decrease in average activation energy of about 5% is noted post-flight.
4 The lowering of the average activation energy of the sensor is most likely due to the lowering of hot pixel activation energy.

ACKNOWLEDGEMENTS

REFERENCES

[1]. A.J.P. Theuwissen, "Influence of Terrestrial Cosmic Rays on the Reliability of CCD Image Sensors-Part 1: Experiments at Room Temperature", IEEE Transactions on Electron Devices, Vol. 54, No. 12, pp. 3260-3266, 2007

[2]. J.F. Ziegler, "Terrestrial cosmic rays", IBM Journal of Research and Development, Vol. 40, No. 1, pp. 19-39, 1996.

[3]. R. Widenhorn et al., "Meyer-Neldel Rule for Dark Current in Charged-Coupled Devices", Journal of Applied Physics, Vol. 89, No. 12, pp. 8179-8182, 2001.

[4]. J.Janesick et al., "Radiation Damage in Scientific Charge-Coupled Devices", IEEE Transactions on Nuclear Science, Vol. 36, No .1, pp.572-578, 1989.

[5]. V.A.J.Van Lint, "The Physics of Radiation Damage in Particle Detectors", Nuclear Instruments and Methods in Physics Research, Vol. A253, No.3, pp. 435-459, 1987

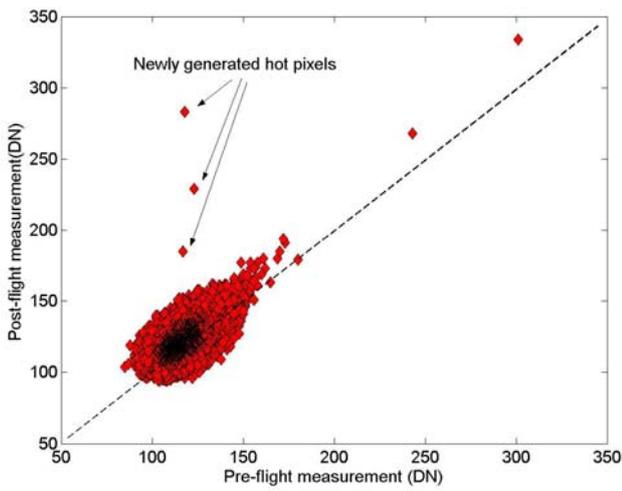[6]. J. Janesick, "Scientific Charge-Coupled Devices", ISBN 0-8194-3698-4, SPIE press, pp.773-774, 2001

Figure 1. Scatter plot comparing pre-flight and post-flight measurements from one test sensor done at 32 °C and 3 second integration time.
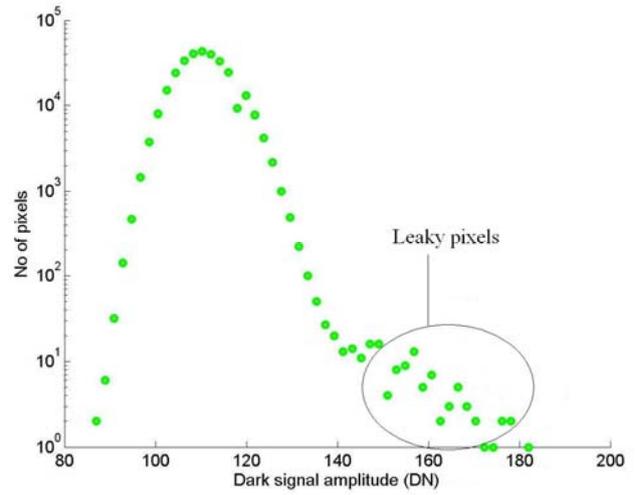

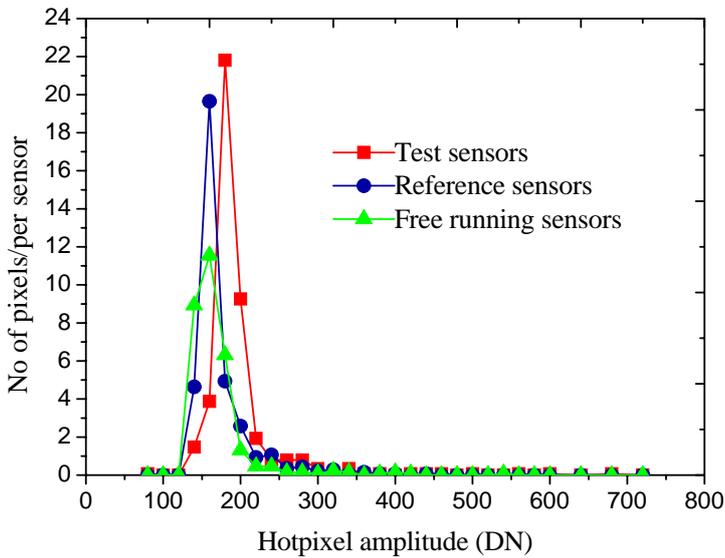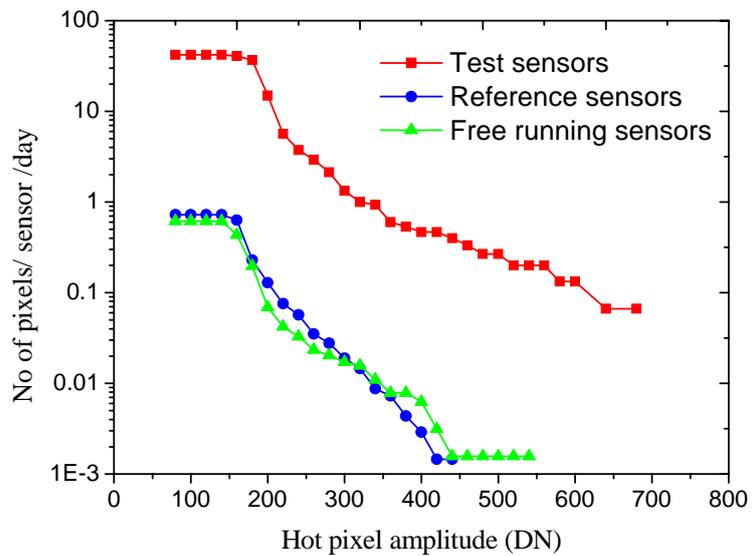Figure 2. Histogram depicting dark signal amplitude (post-flight)

Figure 3. Histogram comparing sensors carried on flight (test sensors), reference sensors kept on the shelf (reference sensors) and sensors kept running on the camera (free running sensors)

Figure 4. Reverse cumulative histogram comparing test sensors, reference sensors and free running sensors.
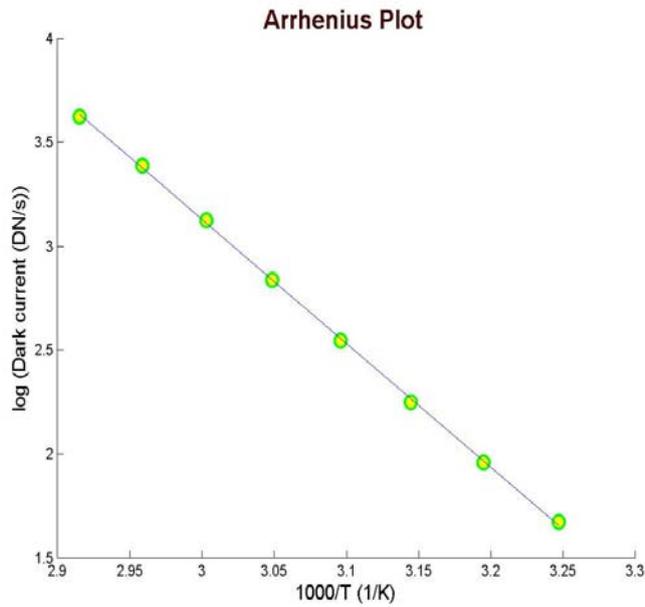
Figure 5. Arrhenius plot of the average dark current

Sensor number	Act. Energy(eV): pre-flight	Act. Energy(eV): post-flight
1	0.60	0.57
2	0.59	0.56
3	0.57	0.54
4	0.59	0.58
5	0.56	0.52
6	0.60	0.58
7	0.58	0.57

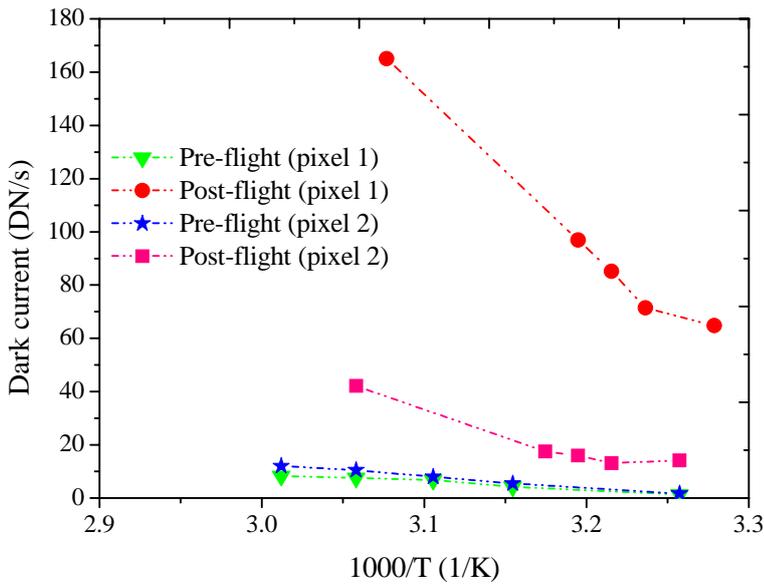Table 1. Comparison of average activation energies of test sensors

Figure 6. Dark current (DN/s) vs. the inverse temperature of two hot pixels pre-flight and post-flight

Activation energy (pixel 1) pre-flight	0.62eV
Activation energy (pixel 1) post-flight	0.41eV
Activation energy (pixel 2) pre-flight	0.61eV
Activation energy (pixel 2) post-flight	0.52eV

Table 2. Activation energies of hot pixels given in figure 6